Experimental investigation of frequency–amplitude decoupling in axial-torsional vibratory pile driving by means of laboratory-scale testing

Gómez, Sergio S.; Tsetas, Athanasios; Meijers, Peter C.; Metrikine, Andrei V.

DOI
10.1016/j.oceaneng.2024.119788

Publication date
2024

Document Version
Final published version

Published in
Ocean Engineering

Citation (APA)
Gómez, S. S., Tsetas, A., Meijers, P. C., & Metrikine, A. V. (2024). Experimental investigation of frequency–amplitude decoupling in axial-torsional vibratory pile driving by means of laboratory-scale testing. *Ocean Engineering*, *316*, Article 119788. https://doi.org/10.1016/j.oceaneng.2024.119788

Ocean Engineering 316 (2025) 119788

Contents lists available at ScienceDirect

Ocean Engineering

journal homepage: www.elsevier.com/locate/oceaneng

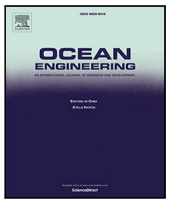

Research paper

Experimental investigation of frequency–amplitude decoupling in axial-torsional vibratory pile driving by means of laboratory-scale testing

Sergio S. Gómez *, Athanasios Tsetas, Peter C. Meijers, Andrei V. Metrikine

Faculty of Civil Engineering and Geosciences, Delft University of Technology, Stevinweg 1, Delft, 2628 CN, The Netherlands

ARTICLE INFO

Keywords:
Vibratory pile driving
Offshore monopiles
Torsional vibrations
Gentle driving of piles
Frequency-amplitude decoupling
Lab experiments

ABSTRACT

This paper presents the development and testing of a lab-scale Gentle Driving of Piles (GDP) shaker. Conventional impact piling for offshore monopile installation faces challenges due to noise regulations and its adverse marine environmental impacts. The GDP method, which integrates high-frequency torsional vibrations with low-frequency axial vibrations, aims to mitigate these issues. In this work, a new GDP shaker is designed and tested to enhance vibratory pile driving by independently controlling torsional and vertical vibration amplitudes and frequencies. Laboratory tests were conducted using the newly designed shaker for pile driving in sandy soil to evaluate its performance. The results indicate a significant reduction in power consumption and improved pile drivability with high-frequency, low-amplitude torsional vibrations. This study highlights the importance of optimizing dynamic inputs for enhanced pile penetration and reduced environmental impact, showcasing the potential of the GDP method as a promising alternative to traditional impact piling techniques.

1. Introduction

The rapid transition from fossil-based to renewable energy sources is becoming increasingly apparent on a global scale (International Energy Agency, 2023). Given this shift, and considering offshore wind as a major source of renewable energy, a major rise in installations of offshore wind turbines is anticipated. To meet the demands of the accelerated energy transition, it is essential to install progressively larger offshore wind farms in deeper waters. This presents several challenges at various levels, with foundation design being one of the most challenging to address. Despite substantial efforts to deploy alternative solutions, such as floating technology capable of operating in deep waters (Musial et al., 2023), monopiles remain the most common type of foundation for both shallow and intermediate water depths, and they are expected to continue being the concept of choice in the future (Ramírez et al., 2021).

The most widely used monopile installation technique, i.e. impact piling, is facing major challenges to meet the requirements regarding noise generation during monopile installation (Tsouvalas, 2020). During impact piling, high-level noise emissions in the water column and seismic waves propagating in the seabed can adversely affect marine species (Bohne et al., 2024). To deal with this problem, in most cases costly and partly efficient noise mitigation measures are employed (Würsig et al., 2000; Koschinski and Lüdemann, 2013), which can also delay the installation process. In the near future, due to the large increase in monopile dimensions, and more importantly in view of the continuous adoption of strict legislation to limit anthropogenic noise in the offshore environment, it is very likely that impact hammering may become infeasible.

Various noise mitigation strategies are presently used to address the environmental concerns associated with impact piling. Most of these approaches aim to extend the impact duration, thereby reducing sound emission levels. This can be achieved for instance by shape optimization of the hammer (Klages et al., 2021). Other examples are the "Blue Piling" technique, which utilizes a large water column to generate the driving force, as well as the MENCK noise reduction unit (MNRU) and the PULSE system of IQIP (Koschinski and Lüdemann, 2020). All these options are based on prolongation of the hammer impact duration and reduction of the impact force, leading to primary noise reduction.

Given the cost and partial efficiency of these measures, the offshore wind industry is actively exploring other alternatives to impact piling, with vibratory techniques being the primary solution to address the associated installation requirements (Holeyman et al., 2020; Staubach et al., 2021; Kaynia et al., 2022). Therefore, established vibration-based methods, such as axial vibratory driving, are currently used as an alternative pile driving technique in offshore construction works. However, the adoption of these techniques in offshore wind projects remains still limited. This is owed to various aspects, related to considerations about the installation (Moriyasu et al., 2018; Tsetas et al., 2023c) and post-installation behaviours (Kementzetzidis et al., 2023b) and open

* Corresponding author.
E-mail address: S.SanchezGomez-1@tudelft.nl (S.S. Gómez).

https://doi.org/10.1016/j.oceaneng.2024.119788
Received 31 July 2024; Received in revised form 8 November 2024; Accepted 12 November 2024
Available online 2 December 2024

questions regarding energy efficiency (Gómez et al., 2022) and sound emissions during vibro-driving (Dahl et al., 2015; Molenkamp et al., 2024). However, there is an additional element related to the questionable capacity of these vibratory tools to drive the large-diameter monopiles up to target depth in an optimal manner.

To provide an alternative solution to impact piling and improve the capabilities of the existing axial vibratory method, the Gentle Driving of Pile (GDP) method was developed (Metrikine et al., 2020). The GDP method is based on the simultaneous application of high-frequency torsional vibrations, as the main driving mechanism, in combination with low-frequency axial vibrations. The high-frequency torsion is introduced with the aim of (i) improving the installation performance, (ii) reducing pile vibrations and thus noise emissions, and (iii) minimizing the disturbance of the surrounding medium. The torsional loading introduces purely shear waves in the surrounding media (Kausel, 2006), which cannot propagate in the seawater fluid (Jensen et al., 2011). Furthermore, it also leads to reduced radial pile expansion (Poisson's effect) due to the small axial vibration amplitudes needed to drive the pile; the latter is the culprit for the noise generated during pile driving. The proof-of-concept of the GDP technique was achieved by building the first GDP shaker and testing piles in terms of both installation and post-installation loading performances against standard driving methods during medium-scale field tests in a sandy soil site (Tsetas et al., 2023a). Even though the GDP method provided promising results with improved drivability and post-installation behaviour (Kementzetzidis et al., 2023a), the use of the standard technology of counter-rotating eccentric masses was recognized as a potential limitation for the method. This is owed to the fact that typically eccentric masses-based vibrators possess a coupling between loading the amplitude and the driving frequency (Wong et al., 1992; Whenham and Holeyman, 2012). In view of this, the next step in the development of the GDP method is focused on the improvement of the shaker design, in a manner that allows the independent control of driving frequency and loading amplitude. To further investigate this topic, new features are included in a new lab-scale GDP shaker, which is utilized to carry out lab-scale pile installation tests and assess its performance.

In this paper, we aim to demonstrate by means of lab-scale tests, the advantages of including additional degrees of freedom to the GDP shaker. To this end, a newly developed lab-scale shaker design is presented that is capable to independently control two modes of vibration, namely torsional and vertical, both in terms of input amplitudes and driving frequencies. A series of pile driving tests are executed in a laboratory environment and data are collected from the instrumented shaker, the pile and the soil. These tests showcase the efficacy of pile driving with torsion at higher frequencies and more importantly, the beneficial effect of the frequency-amplitude decoupling in both installation performance and power consumption. Furthermore, the high-frequency torsion becomes apparent as the main driving mechanism in comparison to vertical vibration. Conclusively, this experimental campaign contributes to the optimization of the GDP technology, by decoupling the frequency and amplitude of axial-torsional vibrations, to further advance sustainable and environmentally friendly monopile installation.

2. Vibratory devices for pile driving

Up to date, there has been a vast development of different types of vibratory devices for onshore pile driving, operating from low-to-medium frequencies (20–40 Hz) to even > 100 Hz; the latter with the aim of operating near the pile-soil-shaker system resonance frequency (Rainer Massarsch et al., 2022). In the case of offshore pile driving, larger-scale vibratory tools are available to install monopile foundations, which operate mostly in the former regime (i.e. around 20–30 Hz). Even though the variable eccentric-moment technology is well-known and has been implemented in existing shakers (Viking, 2002), its adoption is quite limited. Most vibratory tools used in offshore pile driving employ the basic working principle of counter-rotating eccentric masses with fixed eccentricity, which generates a centrifugal force of fixed (nominal) amplitude per frequency. Therefore, the loading amplitude and driving frequency of the input excitation are coupled. This may lead to over-dimensioned vibratory tools and a subsequent increase in underwater noise emissions. Furthermore, this constraint can lead to increased pile fatigue in the case where higher amplitudes (and thus frequency) are required to drive the pile to the target depth, with the risk of pile-tool damage.

Fig. 1. The medium-scale GDP shaker connected to a pile via a bolted flange connection.

Similarly to existing axial vibratory shakers, the dynamic excitation in the original GDP shaker was generated by the counter-rotation of eccentric masses with constant eccentricity. This shaker was powered by means of hydraulic pumps that drove two independent shafts, generating centrifugal forces to induce axial and torsional vibrations; the frequencies and amplitudes of these two excitations were distinct. In particular, one set of eccentrics generated the vertical dynamic load, whereas another set was utilized to generate a resultant torsional moment. The GDP shaker is shown in Fig. 1, being connected to a pile via a flange connection during the GDP field campaign (Tsetas et al., 2023a).

Following the successful execution of the GDP field tests campaign using the GDP shaker (see Fig. 1), a few points of attention were raised related to the frequency–amplitude decoupling to improve the GDP method. The main consideration lies in the proper design of the shaker and its specifications, given the potential high power requirements, and the minimization of super-harmonics that can be quite influential for noise generation. In this manner, the main benefits of the torsional driving mechanism can be fully realized without the need to induce large motion amplitudes to the pile.

2.1. Lab-scale GDP shaker

To investigate the effect of frequency-amplitude decoupling and its potential, a new lab-scale GDP shaker was designed and manufactured (Gómez et al., 2024). Although the scaled shaker is powered by a hydraulic system similar to the original GDP shaker, new features and a different actuation principle have been introduced in the present GDP shaker design.

Table 1
Technical specifications of the hydraulic pistons of the scaled GDP shaker.

Design Pressure [bar]	Weight [kg]	Stroke [mm]	Shaft diameter [mm]
150	1.5	±5	16

Table 2
Summary of the position of the sensors with in the soil container.

Location	Number of sensors PWP [kPa]	Number of sensors SPT [kPa]	Number of sensors Accelerometer [g]	Install. depth [cm]
1a	1	1	2 (X, Y)	30
1b	1	1	2 (X, Y)	60
2a	1	1	3 (X, Y, Z)	30
2b	1	1	2 (X, Y)	60
3	1	1	2 (X, Y)	50
4	1	1	1 (X)	50
5	1	1	–	50
6	1	1	–	50
7a	1	1	1 (X)	30
7b	1	1	–	60
8a	1	1	–	30
8b	1	1	–	60

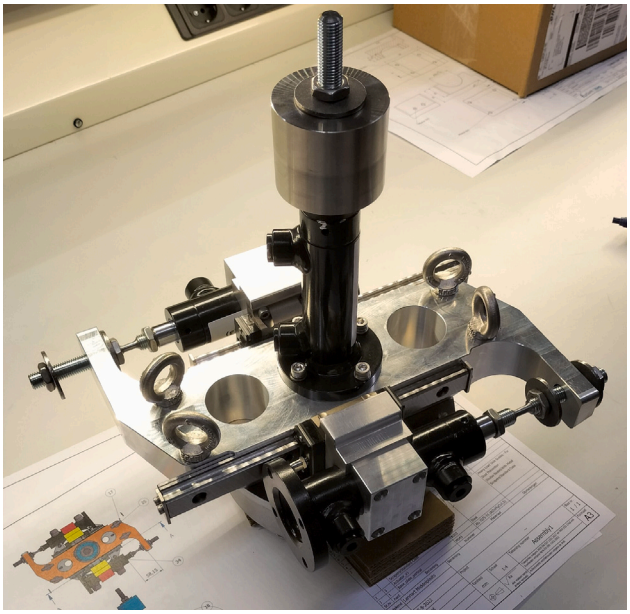

Fig. 2. The newly-developed lab-scale GDP shaker.

The lab-scale shaker consists of a main block made of aluminium of approximately 10 kg to accommodate 3 hydraulic double-acting linear pistons, with a stroke of ±5 mm, that generate the vertical and torsional vibrations (see Fig. 2). Two of the pistons are mounted on the block at diametrically opposite locations and act in opposite directions to generate a dynamic torsional moment. The third piston is mounted in the centre of the shaker perpendicular to the other two pistons and generates the vertical excitation. The shaker is connected to the pile via a friction-based steel clamping component. The design details of the actuators mounted on the shaker are summarized in Table 1.

The shaker is connected to the pile and controlled in a closed feedback loop as shown schematically in Fig. 3. First, the input amplitude and frequency for all actuators is set in the software, generating a sinusoidal signal with the desired amplitude and frequency. The controller then sends the prescribed signal to the valve to generate a harmonic motion, leading to the motion of the pistons and thus the pile excitation. The pistons are hydraulically driven by three fast continuous valves, individually. Furthermore, potentiometers are connected to the actuators, for the purpose of sending a feedback signal to the system and correcting the error by means of a PID controller, to generate the desired signal as accurately as possible. The main new feature of this shaker – compared to the previous design – is the capability to independently prescribe the driving frequency and amplitude in a controlled manner, achieving frequency-amplitude decoupling. The high-level code description of the control system for each individual piston is given in Algorithm 1.

Algorithm 1 Control algorithm for each piston

```
previous_error = 0
integral = 0
for t_i in t do
    set_point = A_p cos(2π f_p t_i)
    error = set_point - measured_value
    proportional = error
    integral = integral + error · Δt
    derivative = (error - previous_error) / Δt
    previous_error = error
    output = K_p · proportional + K_i · integral + K_d · derivative
```

Furthermore, it is noted that the actuation principle of the newly designed shaker is not based on the standard concept of counter-rotating eccentric masses, but on the translational motion of linear hydraulic cylinders with variable added mass. Although this new feature may appear as a minor change, it is a major addition that provides the capability of fast shaker detuning if needed. During pile driving, there is a strong coupling between the pile, the soil, and the shaker. This coupling may lead to undesirable vibrations in the tool that could lead to instability in the controller, which, in turn, could result in damage of tool components and/or large pile vibrations.

3. Description of the experimental set-up

In this section, the lab-scale experimental set-up is presented. In particular, the properties of the shaker, the pile and the soil instrumentation, as well as the process of soil conditioning are described. The main objective of the experimental tests carried out in this work is to investigate the effect of different driving settings in the extended parameter space, owed to frequency-amplitude decoupling. To this end, the newly designed lab-scale shaker is used to drive an instrumented pile into conditioned sandy soil, by means of harmonic input loads with prescribed amplitude and frequency for both motions (torsional and vertical).

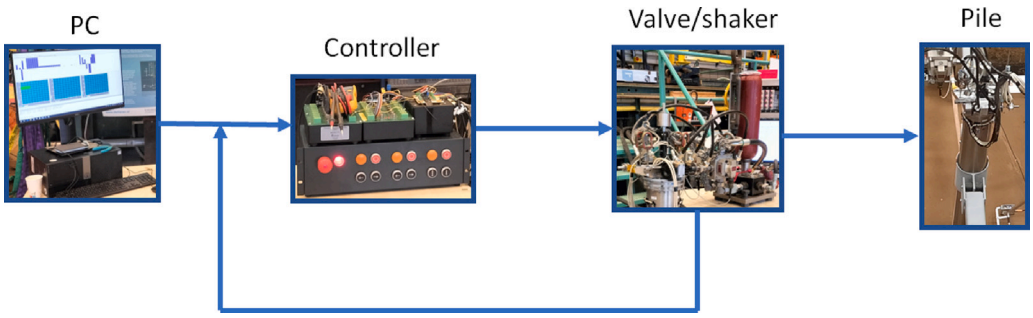

Fig. 3. Feedback control system of the lab-scale GDP shaker.

(a) (b)

Fig. 4. The GeoModel container of dimensions $4 \times 2.5 \times 1.2$ m at the GeoLab of the Deltares facilities in The Netherlands.

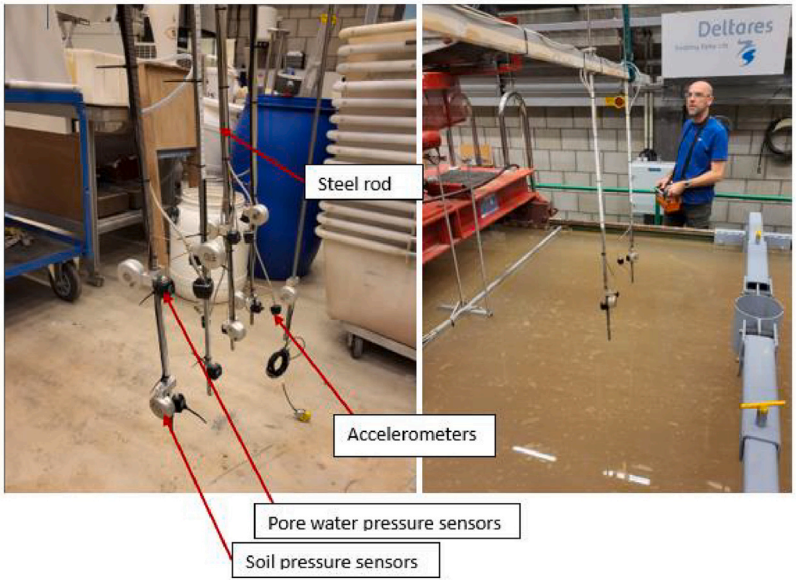

Fig. 5. Pore-water pressure (PWP), soil pressure (SPT) and accelerometers attached on steel rods, prior to placement in the GeoModel container (left) and during placement in the water-saturated sand bed in the GeoModel container (right).

3.1. Soil instrumentation and conditioning

To conduct the pile driving tests, the GeoModel container shown in Fig. 4 located at Deltares (the Netherlands) is utilized (Deltares, Delft, The Netherlands, 2024). The dimensions of the GeoModel container are $4 \times 2.5 \times 1.2$ m ($l \times w \times h$). The container is designed to facilitate the preparation of homogeneous sand profiles with low relative density and is equipped to saturate the soil to the desired level.

To create a homogeneous soil preparation with embedded instrumentation and a desired soil relative density, several steps need to be followed. The first step, prior to filling the GeoModel container with soil, is to instrument the container with pore water pressure

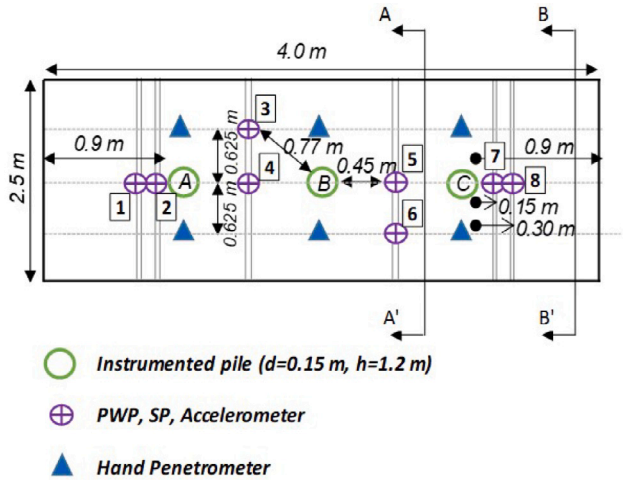

(a) Overview of the soil instrumentation in the GeoModel container.

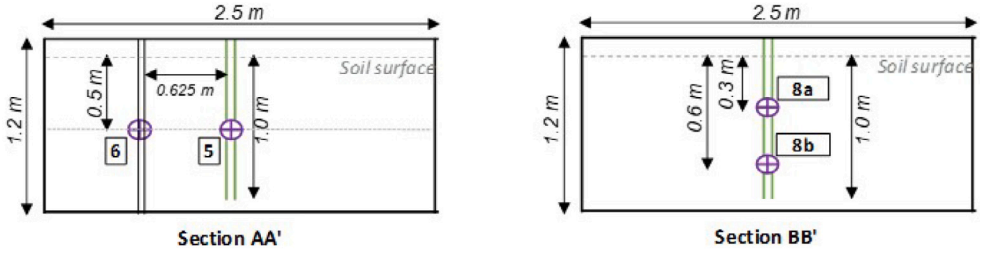

(b) Soil instrumentation at cross-section AA' and BB'.

Fig. 6. Detail description of the soil instrumentation in the GeoModel container consisting of Pore Water Pressure (PWP) and Soil pressure (SP) sensors and accelerometers.

Fig. 7. Water saturation of the sand bed in the GeoModel container.

(a) (b)

Fig. 8. Densification process in two steps: (a) densification with the use of a weight lifted by the crane and hitting the side walls of the container, and (b) densification of the sand bed by using vibrating needles.

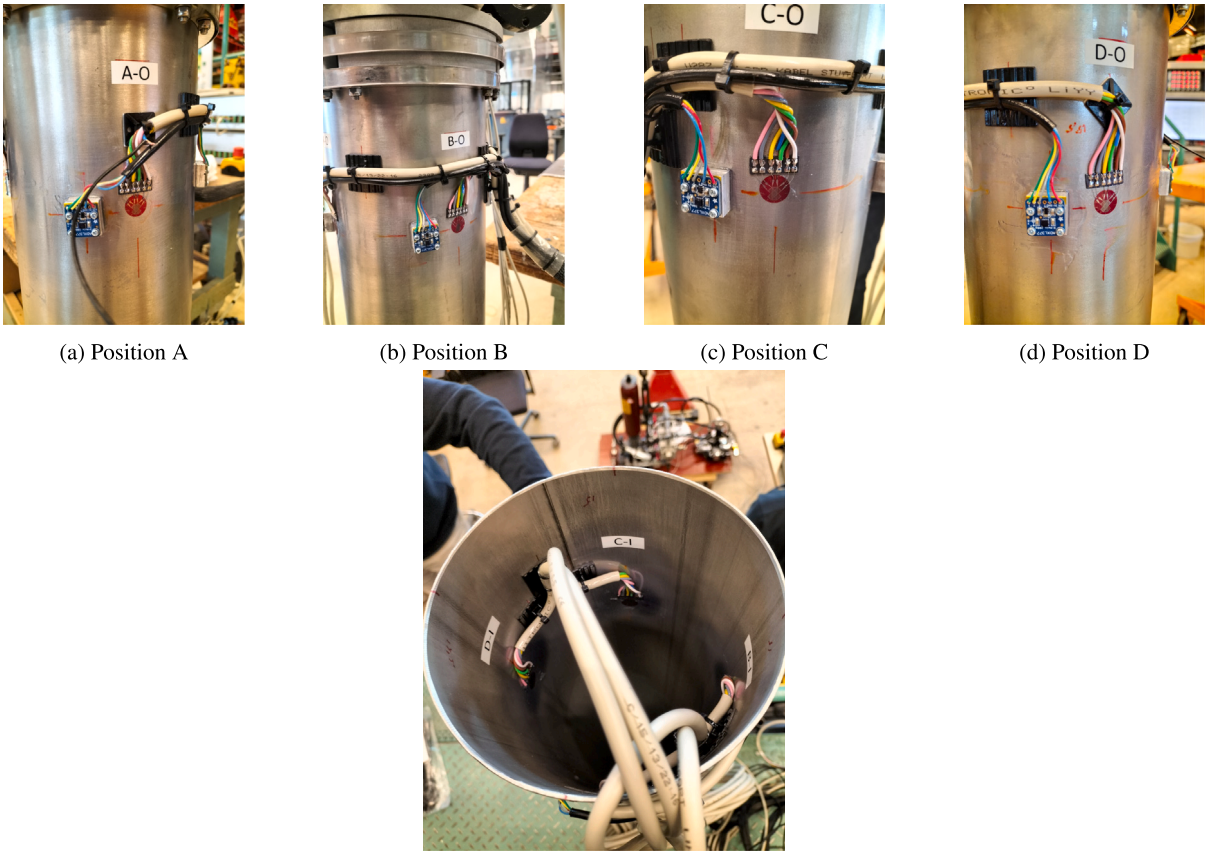

(a) Position A (b) Position B (c) Position C (d) Position D

(e) Inner pile wall instrumentation

Fig. 9. Pile instrumentation consisting of tri-axial accelerometers and strain gauges in rosette configurations.

Table 3
Geometrical and material properties of the test pile.

Material	Length L [mm]	Outer diameter D [mm]	Wall thickness h [mm]
AISI 304	1200	154	2.0

Table 4
Parameter description of the experimental tests for the several soil preparations.

			Torsional		Vertical		Average
			freq. [Hz]	ampl. [mm]	freq. [Hz]	ampl. [mm]	pen.rate [mm/s]
	test	1	0	0	23	≈ 0.8	0.05
	test	2	0	0	23	≈ 1.6	0.16
	test	3	0	0	23	≈ 2.4	0.17
	test	4	0	0	23	≈ 3.3	0.24
	test	5	–	–	–	–	failure
Soil 1	test	6	–	–	–	–	failure
	test	7	30	≈ 0.8	0	0	0.96
	test	8	40	≈ 0.8	0	0	0.52
	test	9	50	≈ 1.0	0	0	0.11
	test	10	60	≈ 1.0	0	0	0.85
	test	11	70	≈ 2.0	0	0	1.06
	test	12	80	≈ 1.5	0	0	0.60
	test	1	0	0	32	≈ 1.4	0.50
Soil 2	test	2	0	0	32	≈ 2.3	2.75
	test	3	69	≈ 2.4	0	0	2.85
	test	1	69	≈ 2.5	23	≈ 1.3	8.50
	test	2	92	≈ 1.2	23	≈ 1.3	0.30
	test	3	92	≈ 1.2	23	≈ 1.3	0.20
Soil 3	test	4	69	≈ 2.5	23	≈ 1.3	0.17
	test	5	69	≈ 2.5	23	≈ 1.3	0.15
	test	6	0	0	23	≈ 3.3	0
	test	7	69	≈ 2.5	0	0	0.13
	test	1	23	≈ 1.4	69	≈ 1.4	4.80
	test	2	23	≈ 2.0	69	≈ 1.4	0.50
Soil 4	test	3	92	≈ 1.2	23	≈ 1.2	0.25
	test	4	92	≈ 1.3	23	≈ 1.2	0.82

Table 5
Properties of Baskarp B20 sand.

Particle density [g/cm^3]	Minimum void ratio [-]	Maximum void ratio [-]
2.641	0.51	0.88

sensors (PWP), soil pressure sensors (SPT) and accelerometers at several locations and depths of the container. In particular, the specific sensors used are as follows:

- Pore pressure sensors of type AKR 1.000 D40 by EPCOS, with a maximum measurement capacity of 100 kPa.
- Soil pressure sensors of type IPT by Kulite, with a maximum measurement capacity of 1100 kPa.
- Triaxial piezoelectric accelerometers of type 830M1 by TE Connectivity, with a measurement range of ± 200 g.

The pore water pressure sensors (PWP) and soil pressure sensors (SPT) were used to measure the evolution of pore pressure and total soil stress, respectively; the latter was measured along the radial direction of the pile. Both SPTs and PWPs are attached to a stiff steel rod. Accelerometers measure accelerations in either one (X), two (X, Y) or three (X, Y, Z) directions simultaneously. The X- and Y-axes correspond to the directions along the long and short edges of the container, respectively, while the Z-axis refers to the vertical direction. Furthermore, all sensors were fully surrounded by soil after installation at the appropriate location. Accordingly, Fig. 5 shows parts of the soil instrumentation process.

The final soil sensor layout is shown in Fig. 6, where A, B and C denote the three pile installation locations. It is noted that the distance between the driving locations is assumed sufficient to not disturb the soil at the different locations during driving (pile-to-pile distance $7D$). Table 2 lists all the sensors installed in the soil, their measurement direction and the embedment depth in correspondence with the labelling shown in Fig. 6.

Next, the GeoModel container is filled with Baskarp B20 sand. First, a loose and homogeneous sand bed is obtained via water saturation. The GeoModel container has two compartments, one for water and the other for sand. In the water compartment, there is a water pump with a manifold connected to several hoses that pump water to the pipes located at the bottom of the sand compartment of the container. These pipes have small orifices that allow the pumped (pressurized) water to uniformly saturate the loose and homogeneous sand preparation from the bottom. The soil saturation process is shown in Fig. 7.

Fig. 10. Shaker detail of strain measurement.

The following step in the set-up preparation is the soil densification. This process is carried out in two steps, (i) application of shock waves on the walls of the container and (ii) dynamic compaction by means of a vibratory needle (see Fig. 8). The shock waves are applied by means of hammering a heavy block onto the side walls of the container. By repeating this several times, and at different locations of the container, a sand bed with a relative density of about 30% can be reached. Fig. 8(a) depicts the densification process by means of impact hammering. To further increase soil density, a vibratory method is used, consisting of a vibrating needle inserted in the soil at a certain depth and slowly pulled out, with a vibration frequency of approximately 192 Hz. The vibrations are effective up to about 30-35 cm in radius of the needle. To obtain a homogeneous sand bed, the vibrator is inserted into the sand and pulled out in multiple locations spaced every 25 cm. Using

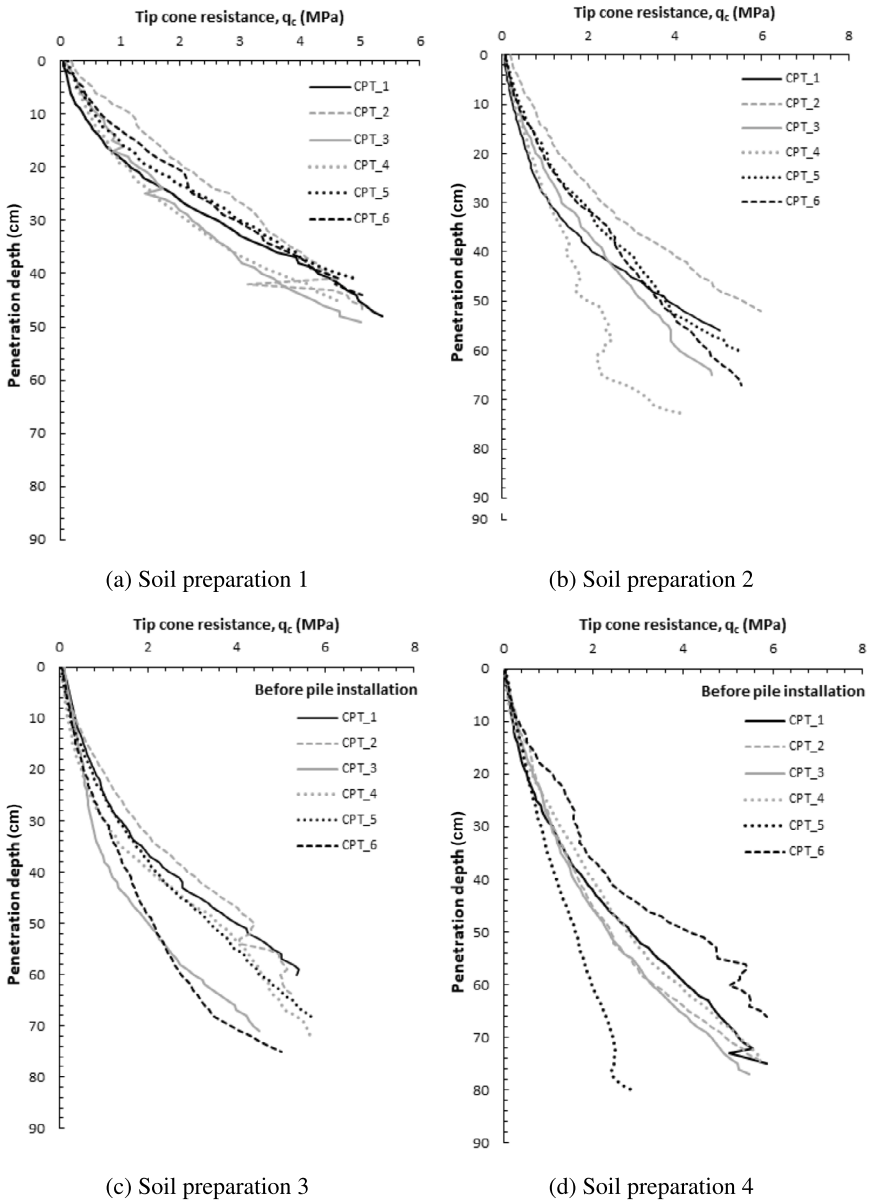

(a) Soil preparation 1

(b) Soil preparation 2

(c) Soil preparation 3

(d) Soil preparation 4

Fig. 11. CPT data for the four soil preparations.

the vibrating needle, a sand bed with a relative density up to 80% can be reached. Fig. 8(b) shows the densification process by vibratory needle. To finalize the soil preparation process and evaluate the final soil conditions, cone penetration tests (CPT) are performed, and soil samples are collected and analysed.

3.2. Pile instrumentation

The test pile material is stainless steel and the pile dimensions are given in Table 3. The choice of pile dimensions was based on two aspects, (i) the geometrical limitations of the GeoModel container, in which the depth of the container bounds the pile embedment and consequently the length of the pile, L, and (ii) the aspect ratios L/D and D/h of the pile, where D is the outer pile diameter and h is the wall thickness; these ratios have been chosen similar to those of large-diameter offshore monopiles.

The test pile is instrumented with four triaxial accelerometers and eight rosette-shaped strain gauges located at the same coordinate (along the pile length), 20 cm from the top of the pile. The accelerometers are installed on the outer wall of the pile, while the strain gauges are installed on both the inner and outer walls as shown in Fig. 9. The specific sensor types are as follows:

- Triaxial accelerometers of type ADXL377 by Analog Devices, with a measurement range of ± 200 g.
- Rosette-shaped strain gauges of type FRAB-6-11 by Tokyo Measuring Instruments Laboratory, with a strain limit of 5%.

The accelerometers are placed equidistant to each other along the circumference (every 90 deg) measuring in three directions (radial, circumferential, and longitudinal). The strain gauges are arranged in a rosette-shape measuring strains along the longitudinal direction of the pile and at ±45 deg to the longitudinal reference strain gauge (see Figs. 9(a) and 9(e)). This instrumentation set-up combining strain and acceleration measurements aims to provide, apart from direct measurement of the respective quantities, the required input to assess accurately the energy flowing to the pile during driving (Gómez et al., 2022).

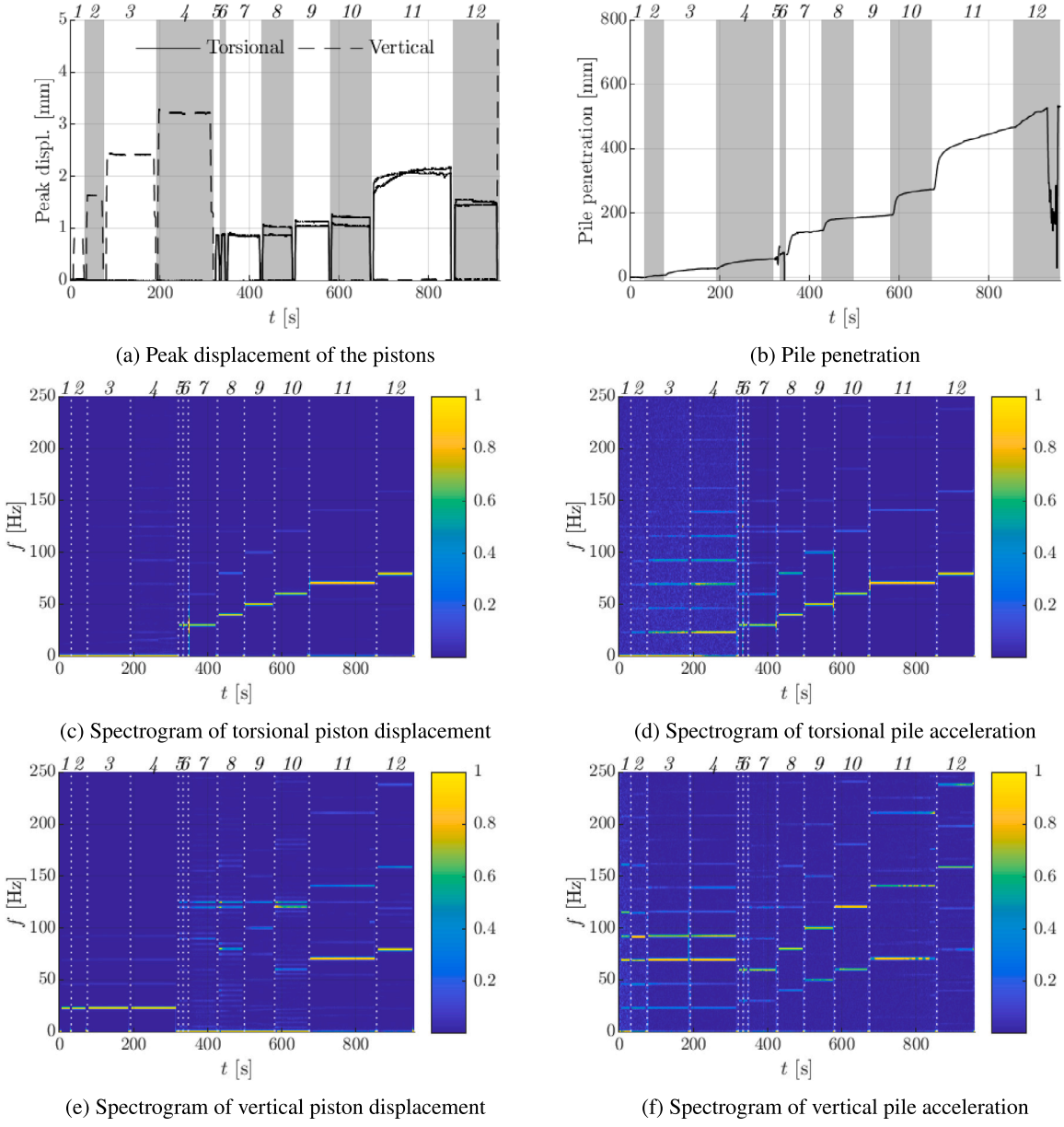

(a) Peak displacement of the pistons

(b) Pile penetration

(c) Spectrogram of torsional piston displacement

(d) Spectrogram of torsional pile acceleration

(e) Spectrogram of vertical piston displacement

(f) Spectrogram of vertical pile acceleration

Fig. 12. Shaker input and pile response data as measured during the tests in soil preparation 1.

3.3. Shaker instrumentation

The dynamic loading transferred to the pile is generated by the motion of the hydraulically driven pistons of the shaker. The loading amplitude can be varied by appending additional mass disks to the flat ends of the piston to certain extent. While the position of the actuators is monitored by the potentiometer that is embedded in the control system, the shaker is further instrumented with two full-bridge strain gauge circuits as shown in Fig. 10 to measure the forces exerted by the pistons; these forces lead to net resultant torsional moment. Finally, the strain gauges are calibrated to provide the load exerted by the pistons at the main block of the shaker.

4. Results

In this section, the results obtained by a wide set of experiments are presented, showcasing the influence of the different shaker parameters (i.e., frequency and amplitude) during installation tests in medium-dense and dense sandy soil. In particular, the tests presented in this work were conducted in four different soil preparations and are summarized in Table 4.

In the following, the results of the experimental tests are presented from measurements on the shaker, the pile and in the soil medium. The test results consist of the torsional and vertical peak amplitudes of the shaker actuators, penetration time series, time–frequency analysis of the pile vibrations and shaker piston motions. Each figure shows a test conducted using different shaker parameters, i.e. frequency and amplitude, for both torsion and vertical excitation in accordance with the description in Table 4. A specific set of parameters is changed whenever a criterion for refusal is met, i.e. pile penetration remains constant for an extended duration.

4.1. Soil characterization

One soil type was used for all tests in the GeoModel container, i.e. the silica sand Baskarp B20 (Sibelco, 2024). The properties of this type of sand are summarized in Table 5. To evaluate the initial state of the soil bed after conditioning, CPTs were conducted consistently at the

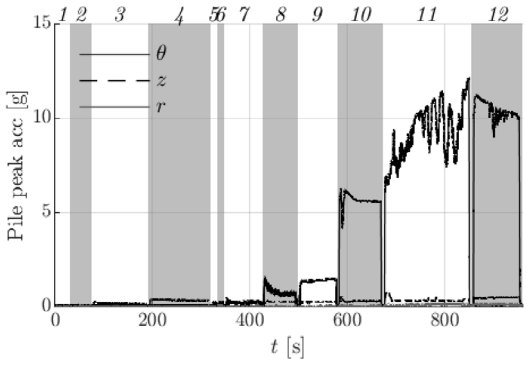

(a) Peak acceleration of the pile in r-, θ- and z-directions.

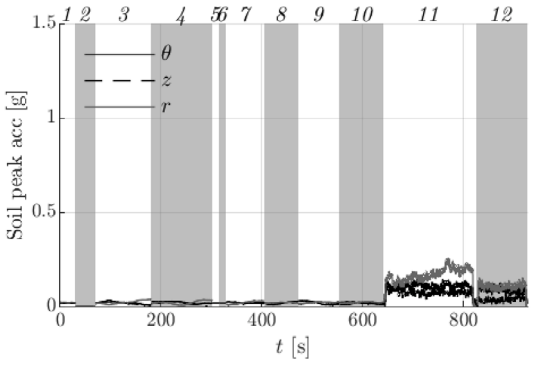

(b) Peak acceleration of the soil in r-, θ- and z-directions.

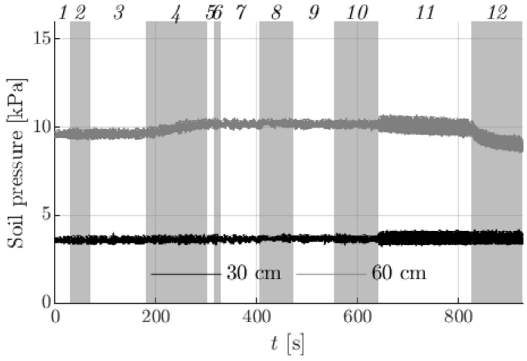

(c) Lateral soil pressure at 30 cm and 60 cm depth.

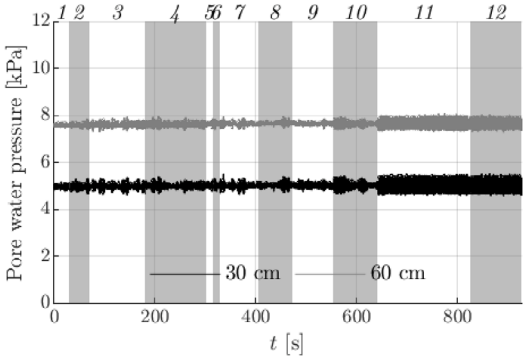

(d) Pore water pressure at 30 cm and 60 cm depth.

Fig. 13. Pile and soil response data as measured during tests in soil preparation 1.

same (six) locations for the four soil preparations. The locations of the tests are shown in Fig. 6(a). The recorded cone tip resistance profiles of the CPTs performed at the different locations are presented in Fig. 11 for the four soil preparations considered in this work.

In general, the obtained CPT profiles present appreciable uniformity for all four soil preparations. In particular, all profiles start from almost zero value at the surface level and increase almost linearly with depth, as expected due to the soil preparation process. Of course, it is anticipated that slightly different cone resistance profiles will occur in some cases. Nonetheless, the CPT results are quite comparable overall, demonstrating a quite (spatially) homogeneous soil preparation.

4.2. Installation tests in soil preparation 1

Fig. 12 shows the effectiveness of the vibration direction (vertical, torsional) at relatively low-frequency and the consequence of increasing the amplitude or the frequency of vibrations. Fig. 12(a) shows the peak amplitude of the shaker actuators in both vertical (dashed lines) and torsional (solid lines) directions. The first four tests are performed at low-frequency (only) vertical vibrations and are accompanied by a progressive increase of the input amplitude. Further on, the vertical vibration is deactivated and the torsional vibration is activated with an initial low frequency (30 Hz), progressively increasing its value up to 60 Hz while the amplitude is kept constant as much as possible and in the low-amplitude range (soil 1; test 7 to test 10). Test 11 shows an increase in amplitude as well as frequency (70 Hz) compared to the previous set of parameters, and to finalize the test, the amplitude is reduced again and the frequency is increased to around 80 Hz.

Fig. 12(b) shows the penetration of the pile as a function of time. This reveals the minor effect of vertical motion and its amplitude increase on drivability. Even though the pile toe is at the soil surface, implying that the soil reaction to driving is close to zero, the pile can penetrate approximately 50 mm into the soil. On the contrary, when low-frequency vibrations are applied in the torsional direction, the penetration rate increases significantly compared to the previous case (test 7). The effect of torsional frequency increase is clearly noticeable in terms of increasing the penetration rate, also in the test where torsional frequency and amplitude are increased (test 11). However, the increase in amplitude is not decisive to avoid pile refusal. This can be observed in the last parameter setting (test 12) where the torsional amplitude is again decreased and the frequency is increased, still led to higher penetration rate compared the previous.

The spectrograms depicted in Figs. 12(c) and 12(e) present the time-frequency analysis of the torsional and vertical input displacement measured at the shaker pistons, while Figs. 12(d) and 12(f) show the averaged amplitude content of the accelerometers on the pile for torsional and vertical motions, respectively. As can be observed in the spectograms, even though the input motion in both torsional and vertical motions is almost monochromatic (content mostly in the fundamental frequency), the response of the pile-soil-shaker system contains super-harmonics with appreciable energy content, which is amplified in the vertical motion. This outcome can result from pile-shaker-soil interaction, and of course from the inherently non-linear system response due to the physics of pile driving (Tsetas et al., 2023b).

Fig. 13 presents the pile and soil accelerations as well as the pore water pressure (PWP) and total stress (SPT) of the soil. The pile accelerations are shown as an average of the four sensors for each measurement direction, namely radial (r), circumferential (θ), and vertical (z). The soil acceleration is measured at location 2a (30 cm deep from the soil surface), and the SPT and PWP are measured at location 2 (see Fig. 6) at two depths, i.e. 30 cm and 60 cm.

For tests 1 to 4, Fig. 13(a) indicates low acceleration levels for all directions with a larger magnitude for the vertical one (black grey line). The vertical acceleration increases with the input amplitude

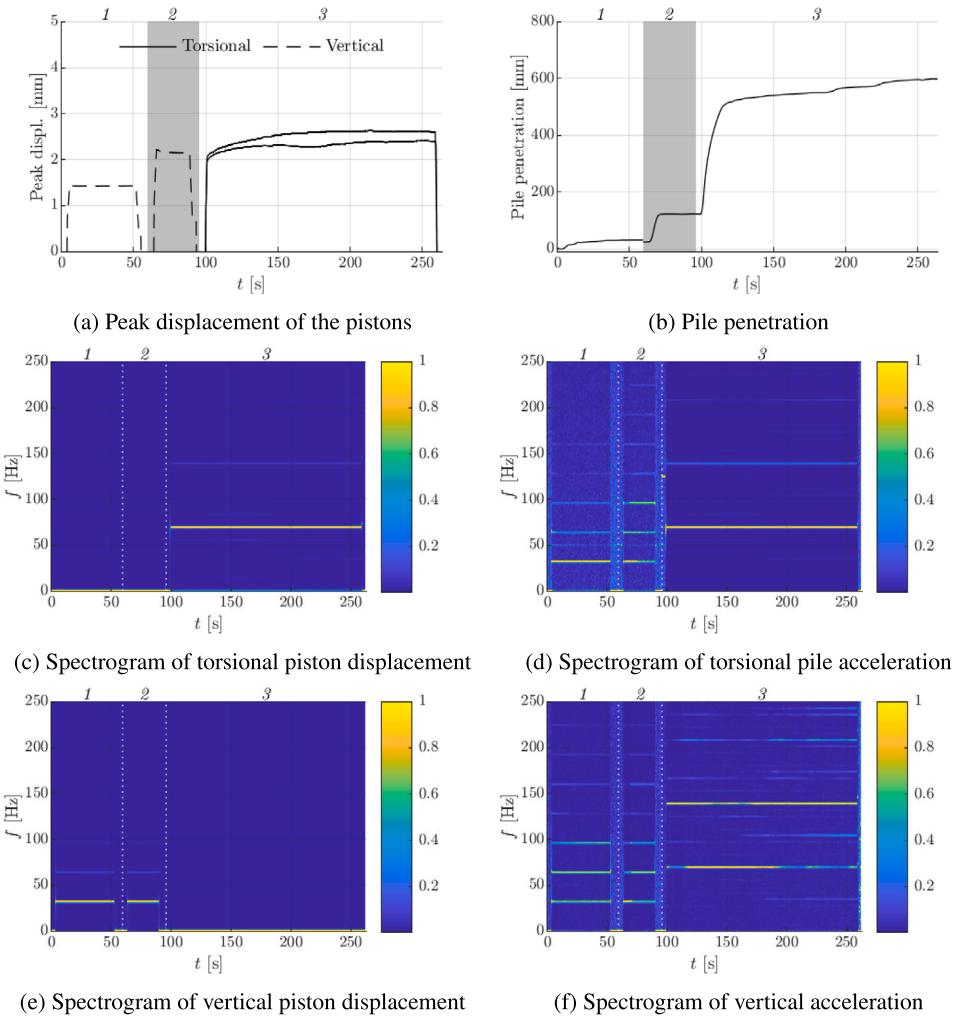

(a) Peak displacement of the pistons

(b) Pile penetration

(c) Spectrogram of torsional piston displacement

(d) Spectrogram of torsional pile acceleration

(e) Spectrogram of vertical piston displacement

(f) Spectrogram of vertical acceleration

Fig. 14. Shaker input and pile response data as measured during the tests in soil preparation 2.

showing weak coupling between directions. The following tests (test 7 to 12) are conducted using only the torsional motion. A substantial increase is observed in the circumferential acceleration and at the same time the input frequency increases strongly compared to test 10. This result indicates the effective energy introduction to the pile at those higher frequencies (60 to 80 Hz). In Fig. 13(b), the soil response is characterized by low acceleration levels compared to pile accelerations at the measured location for the conducted tests in all directions (r, θ and z). The two last tests (test 11 and 12) show a slight increase, even though the relative magnitude compared to the pile acceleration in the θ-direction is still two orders of magnitude lower. Figs. 13(c) and 13(d) plots the soil pressure and pore water pressure dynamic variations at two depths 30 cm and 60 cm.

The test case described in Figs. 12 and 13 showcases the significance of the torsional motion as the main driving mechanism compared to the vertical motion, as well as the effectiveness of torsion with the increase of driving frequency; it is noted that the optimal performance is observed around 70 Hz.

4.3. Installation tests in soil preparation 2

In Fig. 14, and with a new soil preparation, a similar test is performed starting with vertical vibrations only, at similar amplitudes as in the previous case and then activating only the torsional component at a similar amplitude and frequency (69 Hz) of the most effective case in the previous test. Fig. 14(b) shows – as in the previous case – the low effectiveness of the vertical vibrations, as the pile cannot penetrate further than approximately 100 mm. On the contrary, test 3 reveals that the torsional vibrations (only) are most effective around a frequency of 69 Hz with a relatively low amplitude. In this case, the penetration rate of the pile increases drastically and the final penetration target is reached within a few seconds. In Fig. 14(a), the envelopes of the peak displacement measured at the shaker are depicted. In the case of the torsional motion (test 3), a slight mismatch between the torsional actuators, in the order of below 1 mm is measured. This is presumably a result of the pile-soil interaction and the generation of higher harmonics, which can affect the shaker input. Therefore, it is apparent that the PID controller for the input motion of the shaker cannot correct such occurrences at such speed levels. The spectrograms in Figs. 14(c)–14(f), reveal appreciable energy content in the higher frequencies in the vertical direction, especially in the first super-harmonic where the energy intensity is the largest for both sets of amplitudes (among the super-harmonic components). In the test conducted with the torsional vibration only, energy in the vertical direction is also measured given that the pile penetrates vertically thus triggering a frictional coupling even without vertical excitation input.

Fig. 15 shows comparable pile-soil acceleration to the previous test with similar settings. Test 3 presents variability in the pile acceleration, which is caused most likely by a slight asymmetry in the input force. This figure also shows an increase of pile acceleration in the z-direction at the start of each of the three tests and then a deceleration in the z-direction, indicating the pile acceleration in the θ-direction as the

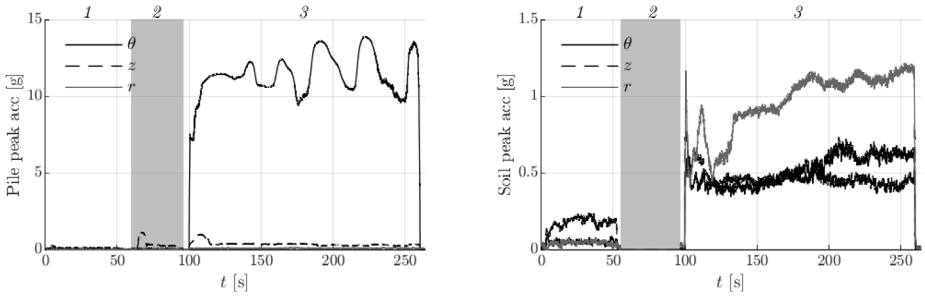

(a) Peak acceleration of the pile in *r*-, *θ*- and *z*-directions.

(b) Peak acceleration of the soil in *r*-, *θ*- and *z*-directions.

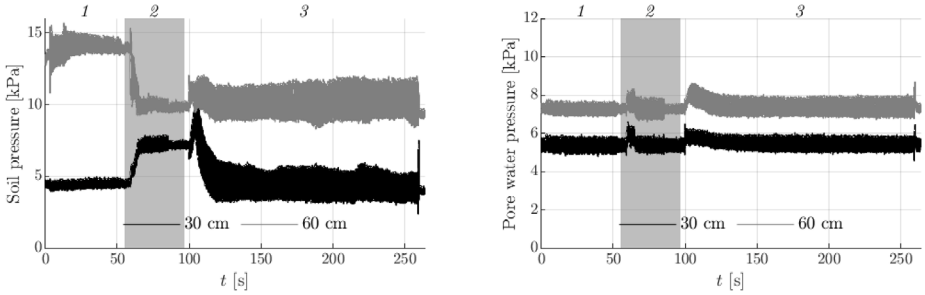

(c) Lateral soil pressure at 30 cm and 60 cm depth.

(d) Pore water pressure at 30 cm and 60 cm depth.

Fig. 15. Pile and soil response data as measured during tests in soil preparation 2.

main pile driving mechanism. Finally, the soil acceleration Fig. 15(b) presents lower acceleration levels compared to the pile, which is an anticipated outcome. Figs. 14 and 15(c) show the soil stress and pore water pressure, where larger variations can be observed compared to the previous case study.

The test results presented in Figs. 14 and 15 showcase the efficacy of the torsional motion in pile penetration at high frequency, even though the amplitude of the shaker pistons is rather small (i.e. in the order of few mm).

4.4. Installation tests in soil preparation 3

The results presented in Fig. 16, correspond to simultaneous low-frequency vertical and high-frequency torsional input of the shaker. In this test, the pile driving behaviour is studied by means of different parameter settings. First, the torsional component is set to 69 Hz while the vertical component is set to 23 Hz, with larger torsional amplitude compared to the vertical one. As expected from the prior test (see Fig. 14), the pile penetrates into the soil with relatively high speed. However, the pile reaches refusal before the desired final penetration depth is reached, thus the penetration speed is close to zero (see Fig. 16(b)). Next, the torsional amplitude is reduced and the torsional frequency is increased up to 92 Hz. As a result, the pile further penetrates into the soil. This alteration demonstrates the effect of torsional frequency increase, while at the same time reducing the torsional vibration amplitude. The effectiveness of concurrent amplitude reduction and frequency increase, testifies that frequency-amplitude decoupling of the input excitation can lead to reduced power requirements without compromising installation performance. Since the final penetration is not yet reached, the torsional amplitude is slightly increased keeping the other parameters (frequency and vertical amplitude) constant. Again, the pile can slightly penetrate with a very low speed. In the next two tests, the torsional frequency is further decreased to the initial 69 Hz, where it can be observed that the pile cannot be further driven into the soil. As a final test, only the vertical shaker is activated at 23 Hz with a relatively large amplitude, without any visible effect on pile penetration. The spectrograms present relatively large energy content in the super-harmonics especially in the vertical motion, which is once again a feature of strong coupling.

Fig. 17 shows the acceleration in the pile, and the pore water pressure and soil stress in the soil. Unfortunately, soil data in test 2 (Soil 3) are not available due to a malfunction in the data acquisition system. Fig. 17(a) showcases that the input amplitude decrease between tests 1 and 2 does not lead to reduced acceleration levels in the pile, yet decreases the accelerations in the soil at the measured location, as shown in Fig. 17(b). The tests conducted in this soil preparation show a quite uniform ratio between pile and soil accelerations throughout the tests.

4.5. Installation tests in soil preparation 4

Fig. 18 presents the experimental results by inverting the GDP method, i.e. low-frequency torsional and high-frequency vertical vibrations. To this end, the vertical motion is set to 69 Hz and the torsional motion to 23 Hz, with the same relatively low amplitude for both motions. In Fig. 18(b), it can be observed that this parameter set leads to a sudden refusal after approximately 40 cm penetration from the initial position of the pile. As a next step, the amplitude of the vertical component is increased. This initiates the penetration with a constant yet lower penetration rate than in the case of the previous parameter set. This appears reasonable given the fact that the soil reaction on the pile should be higher than in its initial position. In the next test, the shaker parameters are changed to the ones corresponding to the original GDP method, i.e. low-frequency vertical motion (23 Hz) and high-frequency torsional motion (92 Hz), with the same relatively low amplitude for both vertical and torsional motions

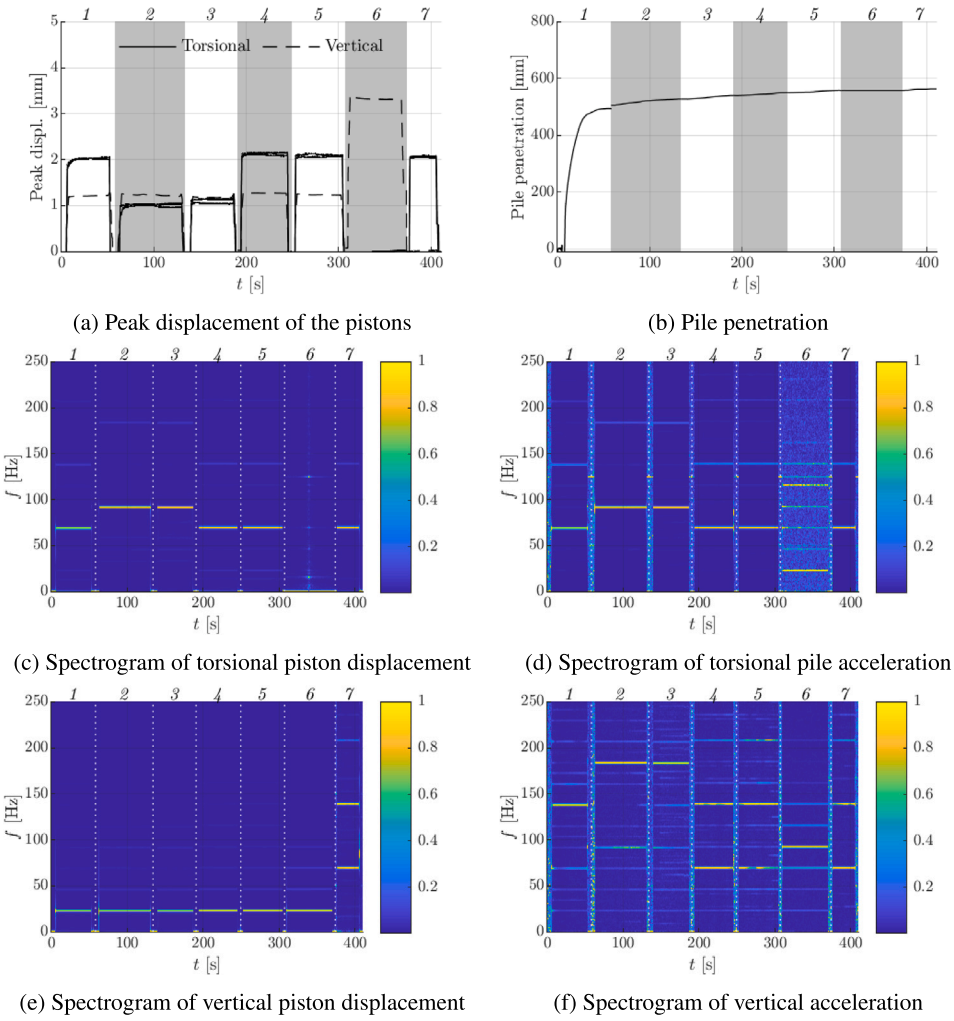

(a) Peak displacement of the pistons

(b) Pile penetration

(c) Spectrogram of torsional piston displacement

(d) Spectrogram of torsional pile acceleration

(e) Spectrogram of vertical piston displacement

(f) Spectrogram of vertical acceleration

Fig. 16. Shaker input and pile response data as measured during the tests in soil preparation 3.

as in the initial test. This set of parameters leads to a restart of the penetration process but refusal is again met almost immediately. As a final step, the torsional amplitude is slightly increased, generating an input force that increases the penetration speed significantly and allows to reach the target penetration depth. As in the test above (Soil 3), the spectrograms show a strong coupling between vertical and torsional motions, especially in the case of low-frequency torsion and high-frequency vertical vibrations.

In Fig. 19 the pile-soil data of the tests performed in soil preparation 4 are depicted. Figs. 19(a) and 19(b) show a strong correlation between pile and soil acceleration magnitudes in the z-direction for tests 1 and 2. In tests 3 and 4, when the GDP method is used, the pile accelerations in θ-direction are substantially increased to approximately ten times larger values than the vertical accelerations in the tests 1 and 2, in which the GDP method is inverted. Although in tests 3 and 4, the vertical frequency is kept at 23 Hz and the amplitude is similar and the torsional frequency is greater than in the case of the inverted GDP method, the soil acceleration is lower than in tests 1 and 2. Likewise, PWP and SPT sensors recorded larger dynamic variations during the tests with the inverted GDP method showing a larger disturbance in the soil.

4.6. Power consumption

To demonstrate the advantageous effect of the input (shaker) frequency-amplitude decoupling for pile driving, the total power consumption is computed. The power P_{cons} is given by:

$$P_{\text{cons}} = F \cdot v, \tag{1}$$

in which F is the total force obtained from the strain measurements at the shaker supporting points and, v represents the velocity, which is obtained by differentiating the displacement with respect to time. Fig. 20 presents the total power consumption based on the measured force and displacement measurements of the three actuators.

In Fig. 20(a) (soil preparation 1), it should be noted that the power increase in the shaker is directly correlated to the penetration speed, especially for tests 11 and 12, also showing a strong coupling between the pile and the shaker. At the same time, the power consumed in the tests 1 to 4 is relatively low compared to the purely torsional tests. Similar conclusions can be drawn with the results obtained by the tests performed with the second soil preparation (soil preparation 2) shown in Fig. 20(b). In Fig. 20(c) (soil preparation 3), an interesting behaviour is observed. In the first test, the GDP method is used to drive the pile into the soil. In test 2, the torsional frequency is increased from 69 to 92 Hz and the amplitude of the torsional actuator is reduced more

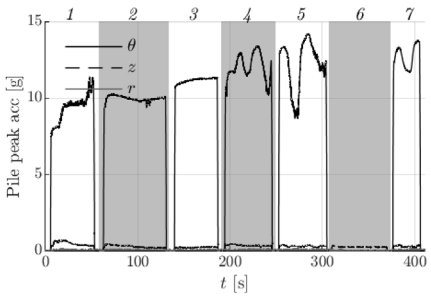

(a) Peak acceleration of the pile in r-, θ- and z-directions.

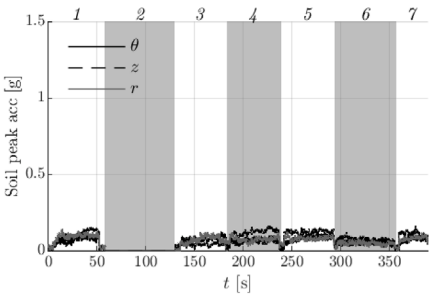

(b) Peak acceleration of the soil in r-, θ- and z-directions.

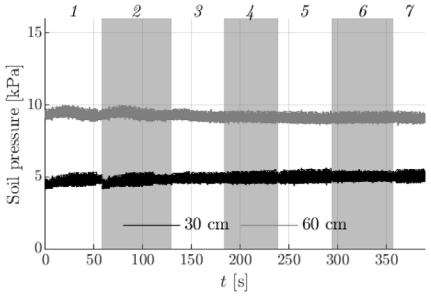

(c) Lateral soil pressure at 30 cm and 60 cm depth.

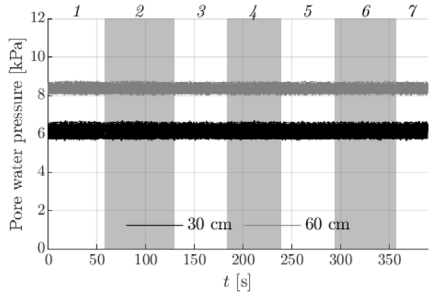

(d) Pore water pressure at 30 cm and 60 cm depth.

Fig. 17. Pile and soil response data as measured during tests in soil preparation 3.

than 50%, resulting in a reduction of the total power consumption and an improvement of the penetration rate. In the following test (test 3), the torsional amplitude is slightly increased improving the penetration speed with still lower consumption than the one calculated in the first test. This observation testifies to the importance of frequency-amplitude decoupling for the shaker power consumption. For soil preparation 4, Fig. 20(d) shows similar power consumption for both the GDP and the inverted GDP method.

It should be noted that the power consumption may not be constant along the penetration given the change in pile-soil resistance. Asymmetries in the power consumption can be explained by a number of factors like the influence of the super-harmonic frequencies in the controllability and asymmetry in the input force due to stiffness imperfections. Overall, the results presented in this section indicate a clear relationship between the input (shaker) parameters and the pile drivability and soil response. It should be pointed out that the torsional motion appears to be most efficient as a driving mechanism at high frequency and relatively low amplitudes. Consequently, the benefits of decoupling the frequency and amplitude of the input loading become apparent.

Overall, the observations of the present work are aligned with previous tests performed with the GDP method. Along with the previous experimental works, a unified numerical modelling framework for both vibratory driving and the GDP method has been developed and validated with field experiments in sand; more details can be found in Tsetas et al. (2023c,a). Through these studies, the synergy of field data and numerical modelling led to deciphering the main driving mechanism of the GDP method, i.e. the redirection of the friction force at the pile–soil interface. In particular, the pile-soil friction is predominantly expended in the circumferential direction and thus reduced soil reaction is encountered along the penetration axis, which leads to enhanced installation performance.

It is noted that the potential reduction in power consumption can offer significant practical benefits in the case of full-scale monopile installations. Lower power requirements translate into cost savings, less deck space coverage in vessels and reduced emissions from installation operations, aligning with both economic and environmental priorities. Additionally, the reduced noise emissions contribute to minimizing the ecological impact on the marine environment, supporting compliance with increasingly strict environmental regulations. These combined advantages position the GDP method as a more sustainable and efficient technology for large-scale offshore wind projects, that can contribute to the achievement of the ambitious offshore wind targets.

5. Conclusions

In this paper, a set of laboratory-scale pile driving tests by means of axial and torsional vibrations are presented (i.e. GDP method). This work focuses on the study of frequency–amplitude decoupling in vibratory pile driving. To this end, a lab-scale shaker was designed and manufactured with independent frequency–amplitude control, and tested in a laboratory environment where small-scale piles were driven in conditioned sandy soil.

The work presented in this paper showcases a clear correlation between input (shaker) parameters with pile drivability and soil response. Moreover, the results of these tests present an appreciable reduction in shaker power consumption accompanied with reasonable pile penetration. This advantageous output is a result of high-frequency dynamics combined with low-amplitude torsional vibrations. Therefore, the experimental observations support that the use of low-amplitude vibrations can lead to increased efficiency in pile driving at higher frequencies, particularly when torsion is used as the main driving mechanism. This major finding highlights the importance of frequency-amplitude decoupling for vibratory driving. It is apparent by the test results that the input amplitude is another parameter that is capable of improving the pile penetration, yet, this has to be in accordance with a proper selection of the overall system dynamic inputs, to bring about benefits in terms of both reduced power consumption but also

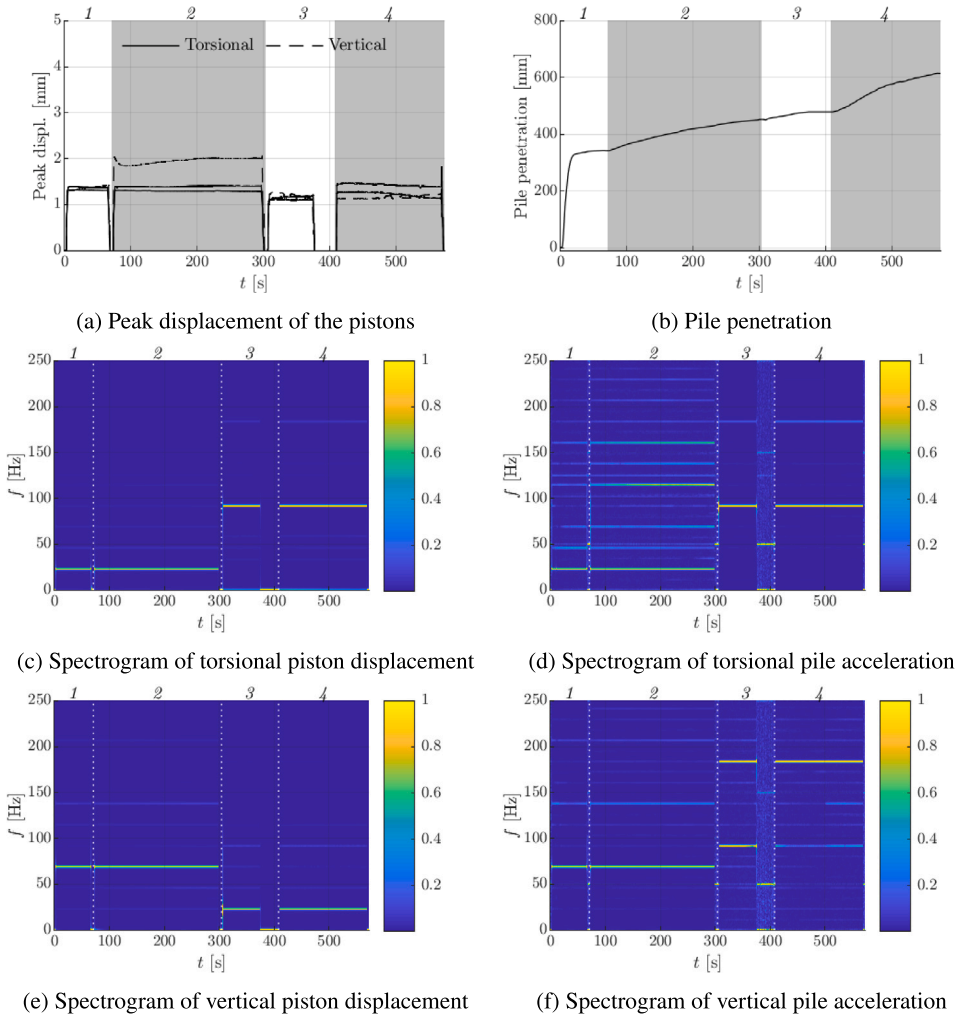

(a) Peak displacement of the pistons

(b) Pile penetration

(c) Spectrogram of torsional piston displacement

(d) Spectrogram of torsional pile acceleration

(e) Spectrogram of vertical piston displacement

(f) Spectrogram of vertical pile acceleration

Fig. 18. Shaker input and pile response data as measured during the tests in soil preparation 4.

improved pile penetration rate. Finally, the time-frequency analyses unveil the presence of super-harmonics of the fundamental frequency both in vertical and torsional motions, with stronger energy content in the vertical direction. The latter indicates that coupling effects between torsional and vertical motions emerge due to pile-soil-shaker interaction.

Towards the future development of the technology, investigating the efficiency of GDP for different soil profiles is essential; recent field tests in clay were successful and dissemination of these findings is part of future work. Offshore testing is also necessary to compare the underwater noise levels of GDP against conventional monopile installation techniques. Finally, designing and manufacturing the GDP shaker for larger monopiles presents its own set of complexities, particularly regarding scalability and controllability at such increased dimensions. Addressing these challenges will be critical for the broader adoption and optimization of GDP for application in offshore wind projects.

CRediT authorship contribution statement

Sergio S. Gómez: Writing – review & editing, Writing – original draft, Visualization, Validation, Resources, Project administration, Methodology, Investigation, Formal analysis, Data curation, Conceptualization. **Athanasios Tsetas:** Writing – review & editing, Validation, Investigation, Formal analysis, Conceptualization. **Peter C. Meijers:** Writing – review & editing, Visualization, Validation, Investigation, Formal analysis. **Andrei V. Metrikine:** Writing – review & editing, Supervision, Funding acquisition.

Declaration of competing interest

The authors declare that they have no known competing financial interests or personal relationships that could have appeared to influence the work reported in this paper.

Acknowledgements

This research is associated with the GDP 1.2 project in the framework of the GROW joint research program. Funding from “Topsector Energiesubsidie van het Ministerie van Econsomische Zaken” under project number HER+-00789470 and financial/technical support from the following partners is gratefully acknowledged: CAPE Holland B.V., Delft Offshore Turbine B.V., EDF Renewables, Eneco Wind B.V., IQIP B.V., RWE Offshore Wind Netherlands B.V., Seaway 7 Offshore Contractors B.V., Shell Global Solutions International B.V., Stichting Deltares, Van Oord Offshore Wind B.V.

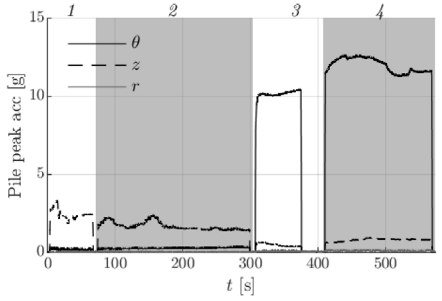

(a) Peak acceleration of the pile in r-, θ- and z-directions.

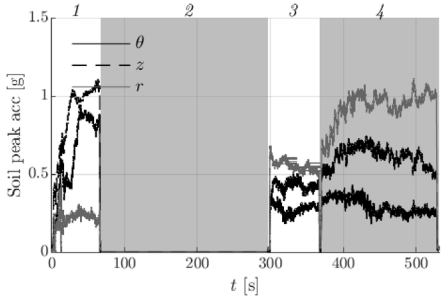

(b) Peak acceleration of the soil in r-, θ- and z-directions.

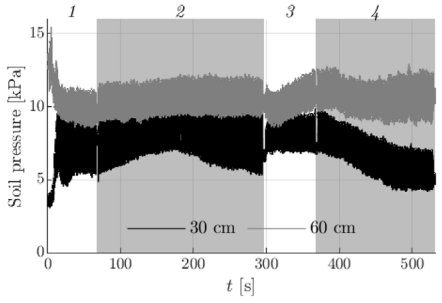

(c) Lateral soil pressure at 30 cm and 60 cm depth.

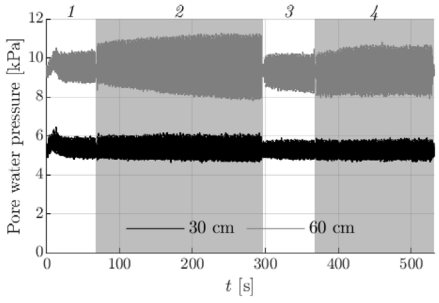

(d) Pore water pressure at 30 cm and 60 cm depth.

Fig. 19. Pile and soil response data as measured during tests in soil preparation 4.

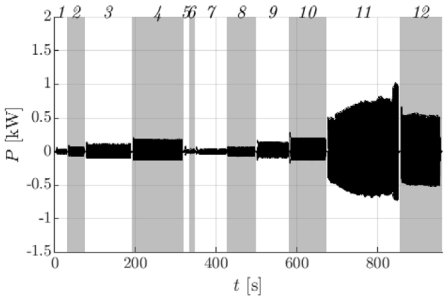

(a) Soil preparation 1.

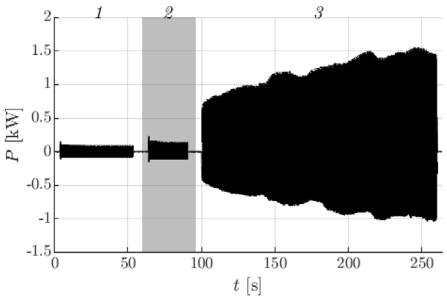

(b) Soil preparation 2.

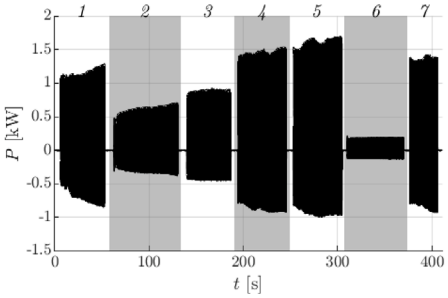

(c) Soil preparation 3.

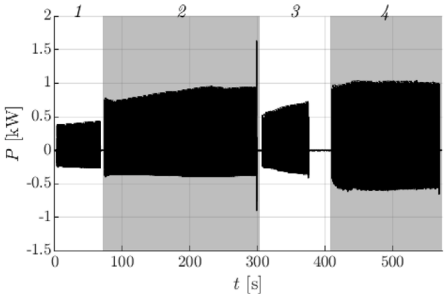

(d) Soil preparation 4.

Fig. 20. Computed power input.

References

Bohne, T., Grießmann, T., Rolfes, R., 2024. Comprehensive analysis of the seismic wave fields generated by offshore pile driving: A case study at the BARD Offshore 1 offshore wind farm. J. Acoust. Soc. Am. 155 (3), 1856–1867. http://dx.doi.org/10.1121/10.0025177.

Dahl, P.H., Dall'Osto, D.R., Farrell, D.M., 2015. The underwater sound field from vibratory pile driving. J. Acoust. Soc. Am. 137 (6), 3544–3554.

Deltares, Delft, The Netherlands, 2024. GeoModel Container. https://project-geolab.eu/geo-model-container-deltares. (Accessed 28 October 2024).

Gómez, S.S., Tsetas, A., Metrikine, A.V., 2022. Energy flux analysis for quantification of vibratory pile driving efficiency. J. Sound Vib. 541, 117299.

Gómez, S.S., Tsetas, A., Middelplaats, L.N., Metrikine, A., 2024. Frequency-amplitude decoupling in the Gentle Driving of Piles (GDP) method: shaker design and experiments. In: Journal of Physics: Conference Series, Vol. 2647, No. 3. IOP Publishing, 032015.

Holeyman, A., Whenham, V., Peralta, P., Ballard, J.-C., Chenicheri Pulukul, S., 2020. Vibratory installation study of a monopile in dense sand. In: International Conference on Offshore Mechanics and Arctic Engineering, Vol. 84423. American Society of Mechanical Engineers, V010T10A014.

International Energy Agency, 2023. World Energy Outlook 2023. Technical Report, Paris, France.

Jensen, F.B., Kuperman, W.A., Porter, M.B., Schmidt, H., Tolstoy, A., 2011. Computational Ocean Acoustics, vol. 794, Springer.

Kausel, E., 2006. Fundamental Solutions in Elastodynamics: A Compendium. Cambridge University Press.

Kaynia, A.M., Hebig, J., Pein, T., Shin, Y., 2022. Numerical model for dynamic installation of large diameter monopiles. Soil Dyn. Earthq. Eng. 161, 107393.

Kementzetzidis, E., Pisanò, F., Elkadi, A., Tsouvalas, A., Metrikine, A., 2023a. Gentle Driving of Piles (GDP) at a sandy site combining axial and torsional vibrations: Part II - cyclic/dynamic lateral loading tests. Ocean Eng. 270, 113452.

Kementzetzidis, E., Pisanò, F., Tsetas, A., Metrikine, A.V., 2023b. Gentle driving of piles at a sandy site combining axial and torsional vibrations: Quantifying the influence of pile installation method on lateral behavior. J. Geotech. Geoenviron. Eng. 149 (11), 04023102.

Klages, E., Lippert, S., von Estorff, O., 2021. A noise-reduced impact hammer for offshore pile driving. In: Proceedings of Meetings on Acoustics, Vol. 44, No. 1. AIP Publishing.

Koschinski, S., Lüdemann, K., 2013. Development of noise mitigation measures in offshore wind farm construction. pp. 1–102, Commissioned by the Federal Agency for Nature Conservation.

Koschinski, S., Lüdemann, K., 2020. Noise Mitigation for the Construction of Increasingly Large Offshore Wind Turbines. Technical Options for Complying with Noise Limits, The Federal Agency for Nature Conservation Isle of Vilm, Germany, p. 40.

Metrikine, A.V., Tsouvalas, A., Segeren, M.L.A., Elkadi, A.S.K., Tehrani, F.S., Gómez, S.S., Atkinson, R., Pisanò, F., Kementzetzidis, E., Tsetas, A., Molenkamp, T., van Beek, K., de Vries, P., 2020. GDP: A new technology for gentle driving of (mono)piles. In: Proceedings of the 4th International Symposium on Frontiers in Offshore Geotechnics. Austin, TX, USA, 16–19 August 2020.

Molenkamp, T., Tsetas, A., Tsouvalas, A., Metrikine, A., 2024. Underwater noise from vibratory pile driving with non-linear frictional pile-soil interaction. J. Sound Vib. 576, 118298.

Moriyasu, S., Kobayashi, S., Matsumoto, T., 2018. Experimental study on friction fatigue of vibratory driven piles by in situ model tests. Soils Found. 58 (4), 853–865.

Musial, W., Spitsen, P., Duffy, P., Beiter, P., Shields, M., Hernando, D.M., Hammond, R., Marquis, M., King, J., Sathish, S., 2023. Offshore Wind Market Report: 2023 Edition. Technical Report, National Renewable Energy Lab.(NREL), Golden, CO (United States).

Rainer Massarsch, K., Wersäll, C., Fellenius, B.H., 2022. Vibratory driving of piles and sheet piles–state of practice. Proc. Inst. Civ. Eng. 175 (1), 31–48.

Ramírez, L., Fraile, D., Brindley, G., 2021. Offshore Wind in Europe: Key Trends and Statistics 2020. WindEurope.

Sibelco, 2024. URL https://www.sibelco.com/en/locations/baskarp.

Staubach, P., Machaček, J., Skowronek, J., Wichtmann, T., 2021. Vibratory pile driving in water-saturated sand: Back-analysis of model tests using a hydro-mechanically coupled CEL method. Soils Found. 61 (1), 144–159.

Tsetas, A., Tsouvalas, A., Gómez, S., Pisanò, F., Kementzetzidis, E., Molenkamp, T., Elkadi, A., Metrikine, A., 2023a. Gentle driving of piles (GDP) at a sandy site combining axial and torsional vibrations: Part I - installation tests. Ocean Eng. 270, 113453.

Tsetas, A., Tsouvalas, A., Metrikine, A.V., 2023b. The mechanics of the Gentle Driving of Piles. Int. J. Solids Struct. 282, 112466.

Tsetas, A., Tsouvalas, A., Metrikine, A.V., 2023c. A non-linear three-dimensional pile–soil model for vibratory pile installation in layered media. Int. J. Solids Struct. 269, 112202. http://dx.doi.org/10.1016/j.ijsolstr.2023.112202.

Tsouvalas, A., 2020. Underwater noise emission due to offshore pile installation: A review. Energies 13 (12), 3037.

Viking, K., 2002. Vibro-Driveability-A Field Study of Vibratory Driven Sheet Piles in Non-Cohesive Soils (Ph.D. thesis). Royal Institute of Technology (KTH).

Whenham, V., Holeyman, A., 2012. Load transfers during vibratory driving. Geotech. Geol. Eng. 30 (5), 1119–1135.

Wong, D., O'Neill, M.W., Vipulanandan, C., 1992. Modelling of vibratory pile driving in sand. Int. J. Numer. Analy. Methods Geomech. 16 (3), 189–210.

Würsig, B., Greene, Jr., C., Jefferson, T., 2000. Development of an air bubble curtain to reduce underwater noise of percussive piling. Mar. Environ. Res. 49 (1), 79–93.